Contribution from the Department of Chemistry,
Harvard University, Cambridge, Massachusetts 02138

Heterometal Cubane-Type Clusters: A $ReFe_3S_4$ Single-Cubane Cluster by Cleavage of an Iron-Bridged Double Cubane and the Site-Voided Cubane $[Fe_3S_4]$ as a Cluster Ligand

Stefano Ciurli[1] and R. H. Holm*

Received July 31, 1990

The reaction of the iron(II)-bridged double-cubane cluster compound $(Et_4N)_2[Re_2Fe_7S_8(SEt)_{12}]$ ($(Et_4N)_2$[**3**]) with 4 equiv of 1,2-bis(dimethylphosphino)ethane (dpme) in acetonitrile affords the single-cubane cluster $(Et_4N)[ReFe_3S_4(SEt)_4(dpme)]$ ((Et_4N)[**4**]) in 72% yield as a black crystalline solid. (Et_4N)[**4**] crystallizes in orthorhombic space group $Pbc2_1$ with a = 12.835 (2) Å, b = 21.260 (4) Å, c = 28.473 (5) Å, and Z = 8. The structure of cluster **4**, which was refined to R (R_w) = 5.22 (5.66)%, reveals the presence of the $[ReFe_3S_4]$ cubane-type core as contained in cluster **3**, with the dmpe ligand bound in a chelating fashion to the Re atom, whose distorted octahedral coordination geometry is completed by an ethanethiolate ligand. The Fe atoms reside in the typical distorted-tetrahedral coordination geometry common to these types of clusters. In the process of bridge cleavage from **3** to **4**, the core oxidation state has been reduced by thiolate from $[ReFe_3S_4]^{4+}$ to $[ReFe_3S_4]^{3+}$. Cluster **4** undergoes two electrochemically reversible processes in acetonitrile solution, which define the three-member core series $[ReFe_3S_4]^{2+,3+,4+}$. The S = 2 ground state of **4** was established by magnetic susceptibility and magnetization measurements. Zero-field Mössbauer spectra were fit with two quadrupole doublets, whose isomer shifts indicate an iron mean oxidation state near $Fe^{2.5+}$, in accord with structural data. Heterometal cubane clusters $[MFe_3S_4]$ of proven structures now include those with M = V, Mo, W, Re, and Ni. Structurally unproven but probable cubane clusters with M = Co, Ni, Zn, and Cd are formed by the reaction of divalent metal ions with protein-bound Fe_3S_4 clusters. These collective results demonstrate an already extensive family of MFe_3S_4 clusters and lead to the concept of the site-voided cuboidal cluster Fe_3S_4 as a semirigid cluster ligand.

Introduction

Research in this laboratory on the synthesis and properties of the heterometal cubane-type clusters MFe_3S_4 was originally directed toward obtainment of a representation of the cluster that is the cofactor of Mo-containing nitrogenases.[2] Bridged double-cubane clusters were prepared by self-assembly reactions, and certain of these were cleaved to single $MoFe_3S_4$ clusters.[3] Analogous WFe_3S_4 clusters have been prepared by similar means.[3,4] Later, a stepwise synthesis of VFe_3S_4 single-cubane clusters was devised.[5] These clusters remain as the best structural models of the molybdenum and vanadium coordination sites in the cofactors and enzymes.[6,7]

The existence of clusters with three different metals, together with certain recent results, suggests that the scope of heterometal MFe_3S_4 cubane-type cluster chemistry is much larger than could have been appreciated when the first few examples of this cluster type were prepared.[3] We are addressing this matter in two ways. First, because all of the foregoing clusters are prepared by self-assembly systems that necessarily involve the appropriate tetrathiometalate $[MS_4]^{z-}$, we have examined systems based on $[ReS_4]^-$.[8,9] This is the only previously known transition-metal $[MS_4]^{z-}$ species whose reactivity as a cluster precursor had not been investigated. In addition, we have recently prepared by a low-temperature method soluble salts of $[NbS_4]^{3-}$ and $[TaS_4]^{3-}$,[10] species otherwise identified only in intractable solids prepared at high temperatures. The reactivity properties of these potential cluster precursors will be reported subsequently.[10] Second, treatment of protein-bound cuboidal Fe_3S_4 clusters with M^{2+} salts affords species whose properties are indicative of the incorporation of M = Co,[11] Ni,[12] Zn,[13,14] or Cd[14] and Fe_3S_4 into a common unit, possibly a MFe_3S_4 cubane. These findings have inspired the synthesis of $NiFe_3Q_4$ clusters (Q = S, Se), whose cubane stereochemistry has been established by X-ray diffraction.[15] Property comparisons strongly support a cubane structure for the protein-bound nickel cluster.[12] Cluster formation with nickel and other biological metals is under continuing study.

The assembly system $[ReS_4]^-/FeCl_2/NaSEt$ in methanol affords three clusters, triply bridged $[Re_2Fe_6S_8(SEt)_9]^{3-}$ (**1**) and Fe^{II}-bridged $[Re_2Fe_7S_8(SEt)_{12}]^{4-}$ (**2**) and $[Re_2Fe_7S_8(SEt)_{12}]^{2-}$ (**3**),[16,17] which contain the cubane-type $ReFe_3S_4$ core and are schematically depicted in Figure 1. As with the analogous molybdenum and tungsten compounds,[3] studies of reactivity and other properties are best performed with single cubanes. This is especially true of electronic aspects inasmuch as intramolecular intercluster magnetic interactions are absent. Here we report the synthesis and the solution and solid state properties of the single-cubane cluster compound $(Et_4N)[ReFe_3S_4(SEt)_4(dmpe)]$ ((Et_4N)[**4**]), thus providing a further contribution to the elucidation of the chemical and physical properties of this class of heteronuclear cubane-type clusters.

Experimental Section

Preparation of Compounds. All operations were carried out at room temperature in an anaerobic atmosphere by using standard Schlenk techniques. Solvents were dried and degassed prior to use. The Et_4N^+ salt of cluster **3** was prepared as described.[17] All other reagents were commercial samples.

$(Et_4N)[ReFe_3S_4(SEt)_4(dmpe)]$ ((Et_4N)[4]). 1,2-Bis(dimethylphosphino)ethane (dmpe, 0.82 mL, 6.2 mmol) was added dropwise to a stirred slurry of $(Et_4N)_2$[**3**] (2.9 g, 1.4 mmol) in 50 mL of acetonitrile. Within 15 min the color changed from orange-brown to green-brown, and all the solid material dissolved. After 36 h a ^1H NMR spectrum of the residue of an aliquot of the reaction mixture revealed 100% conversion

(1) Present address: Institute of Agricultural Chemistry, University of Bologna, 40126 Bologna, Italy.
(2) Holm, R. H. *Chem. Soc. Rev.* **1981**, *10*, 455.
(3) Holm, R. H.; Simhon, E. D. In "Molybdenum *Enzymes*; Spiro, T. G., Ed.; Wiley-Interscience: New York, 1985; Chapter 2.
(4) Christou, G.; Garner, C. D. *J. Chem. Soc., Dalton Trans.* **1980**, 2354.
(5) Kovacs, J.; Holm, R. H. *Inorg. Chem.* **1987**, *26*, 702, 711.
(6) Hedman, B.; Frank, P.; Gheller, S. F.; Roe, A. L.; Newton, W. E.; Hodgson, K. O. *J. Am. Chem. Soc.* **1988**, *110*, 3798 and references therein.
(7) Arber, J. M.; Dobson, B. R.; Eady, R. R.; Hasnain, S. S.; Garner, C. D.; Matsushita, T.; Nomura, M.; Smith, B. E. *Biochem. J.* **1989**, *258*, 733.
(8) Do, Y.; Simhon, E. D.; Holm, R. H. *Inorg. Chem.* **1985**, *24*, 4635.
(9) Müller, A.; Krickemeyer, E.; Bögge, H. *Z. Anorg. Allg. Chem.* **1987**, *554*, 61.
(10) Lee, S. C.; Holm, R. H. *J. Am. Chem. Soc.*, in press, and results to be published.
(11) Moura, I.; Moura, J. J. G.; Münck, E.; Papaefthymiou, V.; LeGall, J. *J. Am. Chem. Soc.* **1986**, *108*, 349.
(12) Conover, R. C.; Park, J.-B.; Adams, M. W. W.; Johnson, M. K. *J. Am. Chem. Soc.* **1990**, *112*, 4562.
(13) Surerus, K. K.; Münck, E.; Moura, I.; Moura, J. J. G.; LeGall, J. *J. Am. Chem. Soc.* **1987**, *109*, 3805.
(14) Münck, E.; Papaefthymiou, V.; Surerus, K. K.; Girerd, J.-J. In *Metal Clusters in Proteins*; Que, L., Jr., Ed.; ACS Symposium Series 372: Washington, DC, 1988; Chapter 15.
(15) Ciurli, S.; Yu, S.-B.; Holm, R. H.; Srivastava, K. K. P.; Münck, E. *J. Am. Chem. Soc.* **1990**, *112*, 8169.
(16) Ciurli, S.; Carney, M. J.; Holm, R. H.; Papaefthymiou, G. C. *Inorg. Chem.* **1989**, *28*, 2696.
(17) Ciurli, S.; Carrié, M.; Holm, R. H. *Inorg. Chem.* **1990**, *29*, 3493.

0020-1669/91/1330-0743$02.50/0

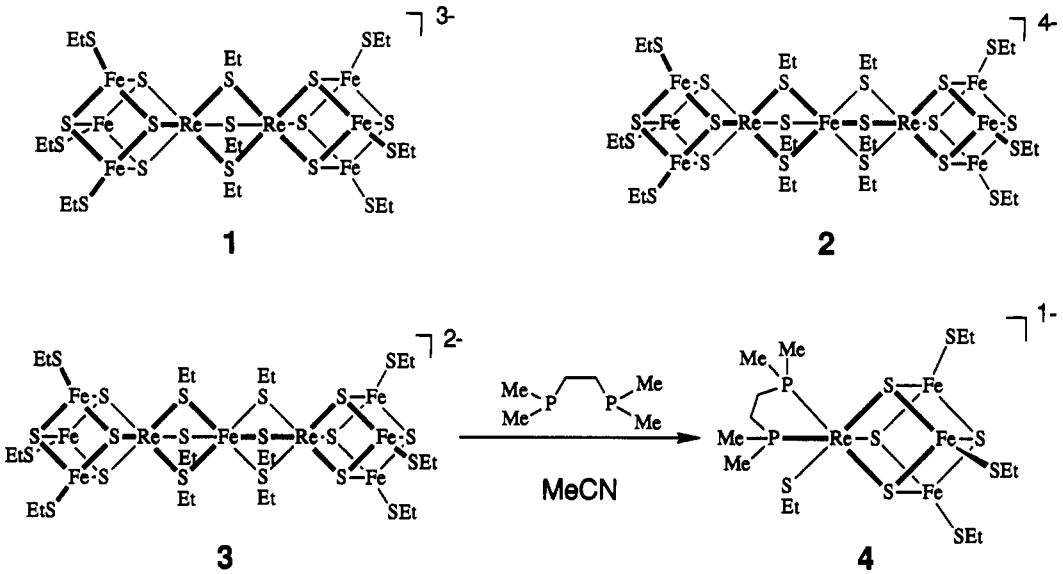

Figure 1. Schematic depiction of $ReFe_3S_4$ double-cubanes **1–3** and the cleavage of **3** by dmpe to afford single-cubane **4**.

of $(Et_4N)_4$[2] to product. This mixture was filtered, the solvent was removed from the filtrate, and the residue was extracted with 100 mL of THF. After addition of ether to the THF solution and storage at −20 °C overnight, 2.1 g (72%) of black crystalline material, pure by ^1H NMR analysis, was collected. An analytical sample was obtained by recrystallization from acetonitrile/ether. Anal. Calcd for $C_{22}H_{56}Fe_3NP_2ReS_8$: C, 26.25; H, 5.61; Fe, 16.64; N, 1.39; P, 6.15; Re, 18.49; S, 25.47. Found: C, 26.49; H, 5.72; Fe, 16.42; N, 1.33; P, 6.74; Re, 17.01; S, 25.11. Absorption spectrum (MeCN): λ_{max} (ϵ_M) 280 (25 300), 397 (16 000) nm. ^1H NMR (298 K, CD_3CN, anion): δ −13.8 (Re-SCH_2), 2.98 (Re-SCH$_2CH_3$), 5.03 (P-Me_a), 5.28 (P-CH_a), 6.64 (Fe′-SCH$_2CH_3$), 7.19 (P-Me_b), 8.45 (Fe″-SCH$_2CH_3$), 8.55 (P-CH_b) 42.7 (Fe′-SCH_2), 64.8, 66.2 (Fe″-SCH_2) ppm.

X-ray Structural Determination. Black plates of (Et_4N)[4] were grown by diffusing ether into an acetonitrile solution at room temperature. One crystal, selected by taking Laue photos on a precession camera, was mounted in a glass capillary and flame-sealed. Data collection was performed at room temperature with a Nicolet P3F four-circle diffractometer equipped with a Mo X-ray source and a graphite monochromator. The orientation matrix and unit cell parameters were determined by the least-squares fit of the angular coordinates of 50 machine-centered reflections with $15° \le 2\theta \le 30°$. Three standard reflections were monitored periodically throughout the course of the data collection, and no decay was observed. Intensity data were corrected for Lorentz and polarization effects by using the program XDISK of the SHELXTL structure determination program package. Empirical absorption corrections were performed with the program XEMP. The compound crystallizes in the orthorhombic system, and the systematic absences $0kl$ ($k \neq 2n$), $h0l$ ($l \neq 2n$), $0k0$ ($k \neq 2n$), and $00l$ ($l \neq 2n$) are consistent with both space groups $Pbc2_1$ (No. 29) and $Pbcm$ (No. 57). Analysis of the E statistics was not decisive in distinguishing between the centro- and the noncentrosymmetric space groups. The space group $Pbc2_1$ was chosen on the basis of the observation that the unit cell parameters are very similar to those of (Et_4N)[$MoFeS_4(SEt)_4$(dmpe)], which crystallizes in this space group.[18]

Structure Solution and Refinement. The structure was solved and refined to low error indices by using the heavy-atom coordinates of the isomorphous compound (Et_4N)[$MoFe_3S_4(SEt)_4$(dmpe)] as starting parameters. All remaining non-hydrogen atoms were located in successive difference Fourier maps and were refined by using SHELXTL. The asymmetric unit consists of two anions and two cations. Some of the carbon atoms belonging to the terminal thiolate groups bound to Fe and to the cation ethyl groups were found to be disordered over two positions and were modeled with equal occupancies. The nondisordered anion atoms were refined anisotropically, and all the remaining atoms were treated isotropically. In the final least-squares cycles, hydrogen atoms were placed 0.96 Å from bonded, nondisordered carbon atoms, with an isotropic temperature factor of 0.08 Å^2. After the last cycle of refinement, each parameter shifted by less than 5% of its esd and the two highest residual peaks were located in the vicinity of the Re atoms. The remaining electron density in the final difference map did not exceed 1.0 e/Å^2. The alternative absolute configuration generated by inverting the coordinates through the origin was rejected on the basis of a Hamilton test.[19] Crystal data are summarized in Table I, and positional parameters are listed in Table II.[20]

Table I. Crystallographic Data for (Et_4N)[$ReFe_3S_4(SEt)_4$(dmpe)]

formula	$C_{22}H_{56}Fe_3NP_2ReS_8$	T, K	298
MW	1006.63	λ, Å	0.710 73 (Mo Kα)
a, Å	12.835 (2)	ρ_{calcd} (ρ_{obsd}),[a] g/cm^3	1.72 (1.72)
b, Å	21.260 (4)		
c, Å	28.473 (5)	μ, cm^{-1}	47.6
space group	$Pbc2_1$ (No. 29)	R, %	5.22
V, Å^3	7769 (2)	R_w, %	5.66
Z	8		

[a] Determined by flotation in dibromomethane/carbon tetrachloride.

Other Physical Measurements. All measurements were performed under anaerobic conditions. ^1H NMR spectra were recorded on a Bruker AM 500 spectrometer. Absorption spectra were obtained with a Cary 219 spectrophotometer. Cyclic voltammetry and coulometry measurements in acetonitrile solutions were performed at room temperature with use of standard PAR instrumentation, a scan rate of 50 mV/s, a Pt-disk working electrode and a Pt-mesh electrode, respectively, an SCE reference electrode, and 0.1 M $(Bu_4N)(ClO_4)$ as the supporting electrolyte. Mössbauer spectroscopic measurements were made at 4.2 and 80 K with the spectrometer operating in the time mode and the source maintained at room temperature. Polycrystalline samples were dispersed in boron nitride powder and sealed in plastic sample holders. Magnetic susceptibility and magnetization measurements at applied fields of 5 kOe and up to 50 kOe, respectively, were carried out using a Quantum Design susceptometer, operating between 1.8 and 300 K. The finely ground polycrystalline sample was packed and weighed into a precalibrated sample holder. The sample holder was then suspended near the center of a plastic straw, which was long enough to be undetected during data collection.

Results and Discussion

The following clusters are of immediate interest in this work:

$[Re_2Fe_6S_8(SEt)_9]^{3-}$	**1**
$[Re_2Fe_7S_8(SEt)_{12}]^{4-}$	**2**
$[Re_2Fe_7S_8(SEt)_{12}]^{2-}$	**3**
$[ReFe_3S_4(SEt)_4(dmpe)]^-$	**4**
$[MoFe_3S_4(SEt)_4(dmpe)]^-$	**5**
$[VFe_3S_4Cl_3(dmpe)(MeCN)]^-$	**6**

Cluster Synthesis. Single-cubane MFe_3S_4 clusters (M = Mo, W) have been prepared by two methods, double-cubane cleavage

(18) Zhang, Y.; Bashkin, J. K.; Holm, R. H. *Inorg. Chem.* **1987**, *26*, 694.

(19) Hamilton, W. C. *Acta Crystallogr.* **1965**, *18*, 502.

(20) See the paragraph at the end of this article concerning supplementary material available.

Table II. Atomic Coordinates ($\times 10^4$) for $[ReFe_3S_4(SEt)_4(dmpe)]^-$

atom	x/a	y/b	z/c
Re(1)	181 (1)	2554 (1)	10736 (1)
Re(2)	5140	5060	9627
Fe(1)	-725 (3)	2707 (1)	11623 (2)
Fe(2)	1393 (3)	2620 (1)	11543 (2)
Fe(3)	343 (3)	3672 (1)	11251 (2)
Fe(4)	6378 (3)	5066 (1)	8831 (2)
Fe(5)	4264 (3)	5184 (1)	8749 (2)
Fe(6)	5405 (3)	6141 (1)	9106 (2)
S(1)	-2079 (6)	2412 (3)	12075 (3)
S(2)	2800 (5)	2122 (3)	11838 (3)
S(3)	485 (6)	4726 (3)	11189 (3)
S(4)	94 (4)	3036 (4)	9968 (4)
S(5)	1692 (4)	3184 (3)	10889 (2)
S(6)	-1160 (5)	3261 (3)	10981 (2)
S(7)	201 (5)	1877 (3)	11404 (3)
S(8)	506 (5)	3302 (3)	12006 (2)
S(9)	7769 (5)	4549 (3)	8544 (3)
S(10)	2892 (7)	4893 (3)	8319 (3)
S(11)	5547 (6)	7182 (3)	9170 (3)
S(12)	5058 (4)	5548 (4)	10445 (4)
S(13)	3841 (5)	5763 (2)	9386 (2)
S(14)	6703 (4)	5632 (2)	9487 (2)
S(15)	5164 (5)	4324 (3)	9008 (3)
S(16)	5508 (5)	5757 (3)	8363 (2)
P(1)	1329 (6)	1831 (3)	10343 (3)
P(2)	-1129 (5)	1843 (3)	10435 (3)
P(3)	3750 (6)	4385 (3)	9970 (3)
P(4)	6226 (6)	4279 (3)	10055 (3)
C(1)	-439 (19)	1128 (12)	10139 (14)
C(2)	531 (16)	1335 (11)	9927 (8)
C(3)	2041 (19)	1240 (9)	10675 (8)
C(4)	2298 (17)	2159 (11)	10001 (14)
C(5)	-2044 (22)	2128 (12)	10026 (13)
C(6)	-2003 (18)	1438 (11)	10834 (10)
C(7)	-2673 (29)	3147 (19)	12266 (18)
C(8)	-3212 (29)	3409 (20)	11939 (19)
C(9)	3795 (22)	2723 (12)	11902 (12)
C(10)	3628 (21)	3151 (13)	12355 (10)
C(11)	-488 (31)	4926 (20)	11484 (20)
C(12)	-1107 (33)	4686 (25)	11945 (23)
C(12')	-1318 (25)	4914 (17)	11681 (15)
C(13)	18 (11)	3881 (9)	10041 (9)
C(14)	263 (21)	4220 (13)	9529 (11)
C(14')	-196 (25)	4196 (16)	9507 (13)
C(15)	5397 (24)	3804 (14)	10292 (14)
C(16)	4307 (17)	3872 (11)	10345 (11)
C(17)	3011 (16)	3915 (10)	9536 (7)
C(18)	2698 (18)	4750 (11)	10323 (9)
C(19)	7162 (20)	4545 (12)	10487 (9)
C(20)	7101 (21)	3818 (14)	9675 (12)
C(21)	8801 (22)	5163 (12)	8513 (12)
C(22)	8784 (22)	5502 (13)	8110 (11)
C(23)	2216 (30)	5641 (20)	8180 (16)
C(24)	1632 (32)	5879 (24)	8509 (18)
C(24')	1511 (33)	5632 (29)	8512 (17)
C(25)	4844 (17)	7501 (10)	8691 (9)
C(26)	3890 (28)	7309 (19)	8630 (18)
C(27)	4979 (20)	6417 (17)	10346 (17)
C(28)	5009 (11)	6768 (10)	10749 (8)

and self-assembly. The double cubanes $[M_2Fe_7S_8(SR)_{12}]^{3-,4-}$ (M = Mo, W), readily prepared in assembly systems and isostructural with **2** and **3** (Figure 1), are cleaved by several reagents. Catechol ($catH_2$) and 3,6-disubstituted catechols (R'_2catH_2) in the presence of base afford $[MoFe_3S_4(SEt)_3Fe(cat)_3]^{3-}$[21] and $[MFe_3S_4(SR)_3(R'_2cat)(solv)]^{2-}$,[22,23] respectively. Cleavage with dmpe gives **5**. Thus far, only catechols and dmpe have been shown to cleave the Fe-bridged clusters with retention of the cubane geometry. The self-assembly systems $[MS_4]^{2-}/FeCl_2/NaS_2CNR_2$ yield the single cubanes $[MFe_3S_4(S_2CNR_2)_5]^-$.[24] In the present work,

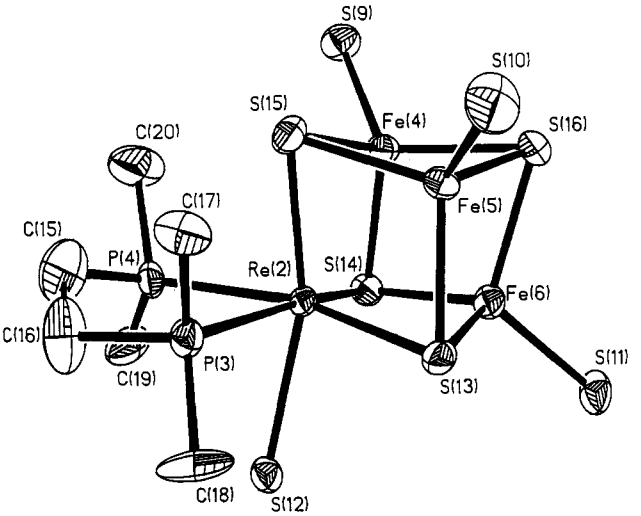

Figure 2. Structure of $[ReFe_3S_4(SEt)_4(dmpe)]^-$ (**4**), showing 30% probability ellipsoids and the atom labeling scheme.

reaction of **2** and **3** with 3,6-diallylcatechol gave only black insoluble material; the self-assembly system containing dithiocarbamate was not investigated.

Treatment of **3** with dmpe in acetonitrile caused complete conversion to **4** in situ (Figure 1), following which (Et_4N)[**4**] was isolated in 72% yield. Dmpe is the only reagent thus far found to produce clean, high-yield cleavage of **3**.[25] In this process, the $[ReFe_3S_4]^{4+}$ core of **3** is reduced to the $[ReFe_3S_4]^{3+}$ level, presumably by thiolate liberated from the bridge during cleavage. Cleavage of **2**, which contains this oxidation level, resulted in partial conversion to **4**, which, however, proved difficult to isolate in pure form. Consequently, double-cubane **3** is the precursor of choice in the preparation of single-cubane **4**.

Structure of $[ReFe_3S_4(SEt)_4(dmpe)]^-$. This cluster has the same overall configuration as **5** and **6**, whose structures have been determined previously.[5,18] Indeed, (Et_4N)[**4**] is isomorphous with (Et_4N)[**5**][18] and contains two inequivalent cluster anions in the asymmetric unit. Anion 2 of cluster **4** is depicted in Figure 2, from which the cubane-type structure is immediately apparent; selected interatomic distance and angle data are compiled in Table III. Clusters **4** and **5** are isostructural and nearly isometric; the principal structural features of **4** are briefly summarized. Bond distances are mean values.

(a) Core Units. The cubane-type core unit is built by the fusion of nonplanar $ReFeS_2$ and Fe_2S_2 rhombs. There is no imposed symmetry, but if the dmpe chelate ring and ethyl group conformations are ignored, the idealized cluster symmetry is C_s. The structures of the $[ReFe_3S_4]^{3+}$ cores in **1**, **2**, and **4** and the $[ReFe_3S_4]^{4+}$ core in **3** are congruent and nearly isometric; in the three isolectronic cores, mean bond distances involving metal atoms differ by no more than 0.04 Å. The structures of **1**–**3** are compared in detail elsewhere.[17] Corresponding core dimensions of the two anions **4** are somewhat irregular, but mean bond distances do not differ by more than 0.04 Å.

(b) The Rhenium Site. The six-coordinate Re atom is tightly integrated in the core, with Re–S distances of 2.389 (6) and 2.36 (2) Å. Terminal coordination is completed by the dmpe chelate ring and one ethanethiolate. The two inequivalent clusters are differentiated in part by their chelate ring conformations. The ring in anion **1**, with methylene carbon atoms C(1) at +0.18 Å

(21) Wolff, T. E.; Berg, J. M.; Holm, R. H. *Inorg. Chem.* **1981**, *20*, 174.
(22) Armstrong, W. H.; Mascharak, P. K.; Holm, R. H. *Inorg. Chem.* **1982**, *21*, 1699; *J. Am. Chem. Soc.* **1982**, *104*, 4373.
(23) Palermo, R. E.; Singh, R.; Bashkin, J. K.; Holm, R. H. *J. Am. Chem. Soc.* **1984**, *106*, 2600.
(24) (a) Liu, Q.-T.; Huang, L.-R.; Kang, B.-S.; Liu, C.-W. *Acta Chim. Sin. (Engl. Ed.)* **1986**, 107. (b) Lei, X.; Huang, Z.; Hong, M.; Liu, Q.; Lin, H. *Jiegou Huaxue (Struct. Chem.)* **1989**, *8*, 152.
(25) A series of potential bridge-cleavage reagents was tested. Reactions of **3** with triazacyclononane yielded mixtures of several unidentified products, whereas MeNC and *t*-BuNC led to the formation of **1**. Reactions with $Na[HB(pz)_3]$ and $K[H_2B(pz)_2]$ afforded $[Fe_4S_4(SEt)_4]^{2-}$ and a mixture of **1** and **2**, respectively. No reaction with $Me_2NCH_2CH_2NMe_2$ was observed, whereas **2** was formed with 2,2'-bipyridyl.

Table III. Selected Interatomic Distances (Å) and Angles (deg) for $[ReFe_3S_4(SEt)_4(dmpe)]^-$

Distances

anion 1		anion	
Re(1)···Fe(1)	2.797 (4)	Re(2)···Fe(4)	2.766 (4)
Re(1)···Fe(2)	2.776 (4)	Re(2)···Fe(5)	2.754 (4)
Re(1)···Fe(3)	2.798 (3)	Re(2)···Fe(6)	2.755 (3)
mean	2.79 (1)	mean	2.758 (7)
Fe(1)···Fe(2)	2.734 (5)	Fe(4)···Fe(5)	2.734 (5)
Fe(1)···Fe(3)	2.684 (5)	Fe(4)···Fe(6)	2.719 (4)
Fe(2)···Fe(3)	2.741 (5)	Fe(5)···Fe(6)	2.705 (5)
mean	2.72 (3)	mean	2.72 (1)
Re(1)-P(1)	2.408 (7)	Re(2)-P(3)	2.494 (7)
Re(1)-P(2)	2.418 (7)	Re(2)-P(4)	2.490 (7)
mean	2.413 (7)	mean	2.492 (3)
Re(1)-S(5)	2.396 (6)	Re(2)-S(13)	2.343 (6)
Re(1)-S(6)	2.388 (6)	Re(2)-S(14)	2.379 (6)
Re(1)-S(7)	2.384 (7)	Re(2)-S(15)	2.356 (7)
mean	2.389 (6)	mean	2.36 (2)
Re(1)···S(8)	3.973 (7)	Re(2)···S(16)	3.921 (7)
Re(1)-S(4)	2.418 (1)	Re(2)-S(12)	2.536 (1)
Fe(1)-S(6)	2.244 (8)	Fe(4)-S(14)	2.261 (7)
Fe(1)-S(7)	2.218 (7)	Fe(4)-S(15)	2.272 (8)
Fe(1)-S(8)	2.300 (7)	Fe(4)-S(16)	2.277 (7)
Fe(2)-S(5)	2.246 (7)	Fe(5)-S(13)	2.259 (7)
Fe(2)-S(7)	2.234 (7)	Fe(5)-S(15)	2.284 (8)
Fe(2)-S(8)	2.269 (7)	Fe(5)-S(16)	2.289 (7)
Fe(3)-S(5)	2.266 (7)	Fe(6)-S(13)	2.304 (7)
Fe(3)-S(6)	2.252 (7)	Fe(6)-S(14)	2.264 (7)
Fe(3)-S(8)	2.300 (8)	Fe(6)-S(16)	2.269 (8)
mean	2.26 (3)	mean	2.27 (1)
Fe(1)-S(1)	2.252 (9)	Fe(4)-S(9)	2.250 (7)
Fe(2)-S(2)	2.255 (7)	Fe(5)-S(10)	2.233 (9)
Fe(3)-S(3)	2.256 (7)	Fe(6)-S(11)	2.229 (6)
mean	2.254 (2)	mean	2.24 (1)

Angles

anion 1		anion 2	
P(1)-Re(1)-P(2)	82.0 (2)	P(3)-Re(2)-P(4)	79.7 (2)
S(5)-Re(1)-S(6)	100.3 (2)	S(13)-Re(2)-S(14)	102.9 (2)
S(4)-Re(1)-S(7)	167.7 (3)	S(12)-Re(2)-S(15)	162.7 (3)
P(1)-Re(1)-S(7)	88.8 (2)	P(3)-Re(2)-S(15)	85.6 (2)
P(2)-Re(1)-S(7)	84.9 (2)	P(4)-Re(2)-S(15)	85.4 (2)
P(1)-Re(1)-S(5)	86.9 (2)	P(3)-Re(2)-S(13)	88.6 (2)
P(2)-Re(1)-S(6)	89.8 (2)	P(4)-Re(2)-S(14)	87.2 (2)
S(5)-Re(1)-S(7)	100.6 (2)	S(13)-Re(2)-S(15)	102.3 (2)
S(6)-Re(1)-S(7)	99.0 (2)	S(14)-Re(2)-S(15)	101.7 (2)
P(1)-Re(1)-S(4)	82.9 (3)	P(3)-Re(2)-S(12)	81.2 (3)
P(2)-Re(1)-S(4)	84.9 (3)	P(4)-Re(2)-S(12)	81.4 (3)
S(4)-Re(1)-S(5)	88.0 (2)	S(12)-Re(2)-S(13)	88.5 (2)
S(4)-Re(1)-S(6)	87.9 (2)	S(12)-Re(2)-S(14)	88.6 (2)
S(6)-Fe(1)-S(7)	108.8 (3)	S(14)-Fe(4)-S(15)	108.3 (3)
S(7)-Fe(1)-S(8)	101.8 (3)	S(15)-Fe(4)-S(16)	104.0 (3)
S(6)-Fe(1)-S(8)	105.6 (2)	S(14)-Fe(4)-S(16)	103.3 (2)
S(5)-Fe(2)-S(7)	110.3 (3)	S(13)-Fe(5)-S(15)	107.4 (3)
S(5)-Fe(2)-S(8)	103.1 (2)	S(13)-Fe(5)-S(16)	105.2 (2)
S(7)-Fe(2)-S(8)	102.2 (3)	S(15)-Fe(5)-S(16)	103.2 (3)
S(5)-Fe(3)-S(6)	108.8 (3)	S(13)-Fe(6)-S(14)	108.0 (3)
S(5)-Fe(3)-S(8)	101.5 (3)	S(13)-Fe(6)-S(16)	104.4 (3)
S(6)-Fe(3)-S(8)	105.3 (3)	S(14)-Fe(6)-S(16)	103.4 (3)
Re(1)-S(5)-Fe(2)	73.4 (2)	Re(2)-S(13)-Fe(5)	73.5 (2)
Re(1)-S(5)-Fe(3)	73.7 (2)	Re(2)-S(13)-Fe(6)	72.8 (2)
Fe(2)-S(5)-Fe(3)	74.8 (2)	Fe(5)-S(13)-Fe(6)	72.7 (2)
Re(1)-S(6)-Fe(1)	74.2 (2)	Re(2)-S(14)-Fe(4)	73.1 (2)
Re(1)-S(6)-Fe(3)	74.1 (2)	Re(2)-S(14)-Fe(6)	72.8 (2)
Fe(1)-S(6)-Fe(3)	73.3 (2)	Fe(4)-S(14)-Fe(6)	73.9 (2)
Re(1)-S(7)-Fe(1)	74.8 (2)	Re(2)-S(15)-Fe(4)	73.4 (2)
Re(1)-S(7)-Fe(2)	73.8 (2)	Re(2)-S(15)-Fe(5)	72.9 (2)
Fe(1)-S(7)-Fe(2)	75.8 (2)	Fe(4)-S(15)-Fe(5)	73.7 (3)
Fe(1)-S(8)-Fe(2)	73.5 (2)	Fe(4)-S(16)-Fe(5)	73.6 (2)
Fe(1)-S(8)-Fe(3)	71.4 (2)	Fe(4)-S(16)-Fe(6)	73.4 (2)
Fe(2)-S(8)-Fe(3)	73.7 (2)	Fe(5)-S(16)-Fe(6)	72.8 (2)

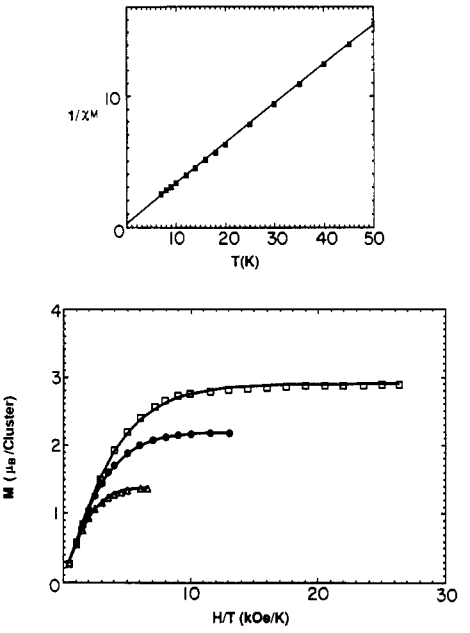

Figure 3. Magnetic properties of cluster **4**. The upper plot shows the temperature dependence of the inverse molar susceptibility $(emu/mol)^{-1}$; the solid line through the data is a fit to the Curie–Weiss law using the parameters in Table V. The lower plot shows the magnetization vs H/T at, from top to bottom, H = 50, 25, and 12.5 kOe; solid lines are fits to the data using the parameters in Table V.

and C(2) at −0.48 Å relative to the Re(1)P(1,2) plane and a P(1)–C(2)–C(1)–P(2) dihedral angle of 48.1°, has the "asymmetric" skew or near-"half-chair" conformation.[26] In anion 2 (Figure 2), the corresponding carbon atoms are more nearly planar; C(15) is at +0.01 Å, C(16) is at −0.22 Å, and the dihedral angle is 21.5°, leading to the asymmetric envelope conformation.[26] Apparently associated with the conformations are distinctly different Re–P and Re–SEt distances in the two anions, although the specific interactions responsible for them are unclear. Very similar structural features have been found for the two independent anions in the structure of (Et_4N)[**5**].[18] The Re–P distances of **4** may be compared with those $Re^{I,III}$–dmpe and related species,[27-29] including *trans*-$[Re(dmpe)_2Cl_2]^+$ (2.438 (2) Å). Similarly, the Re–SEt bond lengths of **4** are found to be somewhat longer than Re^V–SR bonds (R = alkyl, aryl) in five- or six-coordinate complexes (range 2.30–2.35 Å).[30] These results suggest an effective oxidation state in the Re^{III}–Re^V range.

(c) The Iron Sites. Each site contains an approximately tetrahedral $FeS_3(SEt)$ unit. Terminal bond lengths in these units are responsive to the Fe (mean) oxidation state and increase with increasing Fe^{II} character. The values in **4** (2.254 (2), 2.24 (1) Å) indicate a higher oxidation state than in $[Fe_4S_4(SEt)_4]^{3-}$ ($Fe^{2.33+}$, 2.324 (5) Å[31]) and other $[Fe_4S_4(SR)_4]^{3-}$ clusters (range 2.27–2.32 Å[31-33]). They do not reach the value of $[Fe_4S_4(SR)_4]^-$ ($Fe^{2.75+}$, 2.21 Å[34]). They are typical of $[Fe_4S_4(SR)_4]^{2-}$ species[32,33]

(26) Hawkins, C. J. *Absolute Configurations of Metal Complexes*; Wiley-Interscience: New York, 1971; pp 9–10. A negative displacement is in the direction of the S(4) or S(12) atom of the ethanethiolate ligands.
(27) $[Re(dmpe)_2Cl_2]^+$: Vanderheyden, J.-L.; Heeg, M. J.; Deutsch, E. *Inorg. Chem.* **1985**, *24*, 1666.
(28) $[Re(depe)_2Cl_2]^+$: Cotton, F. A.; Daniels, M. L. *Inorg. Chim. Acta* **1988**, *142*, 255 (depe = 1,2-bis(diethylphosphino)ethane).
(29) $[Re(dmpe)_2H(PPh_2)]$: Jones, W. D.; Maguire, J. A. *Organometallics* **1987**, *6*, 1728.
(30) Blower, P. J.; Dilworth, J. R.; Hutchinson, J. P.; Nicholson, T.; Zubieta, J. *J. Chem. Soc., Dalton Trans.* **1986**, 1339; *Inorg. Chim. Acta* **1984**, *90*, L27.
(31) Hagen, K. S.; Watson, A. D.; Holm, R. H. *Inorg. Chem.* **1984**, *23*, 2984.
(32) Berg, J. M.; Holm, R. H. In *Iron-Sulfur Proteins*; Spiro, T. G., Ed.; Wiley-Interscience: New York, 1982; Chapter 1.
(33) Carney, M. J.; Papaefthymiou, G. C.; Spartalian, K.; Frankel, R. B.; Holm, R. H. *J. Am. Chem. Soc.* **1988**, *110*, 6084 and references therein.
(34) O'Sullivan, T.; Millar, M. M. *J. Am. Chem. Soc.* **1985**, *107*, 4096.

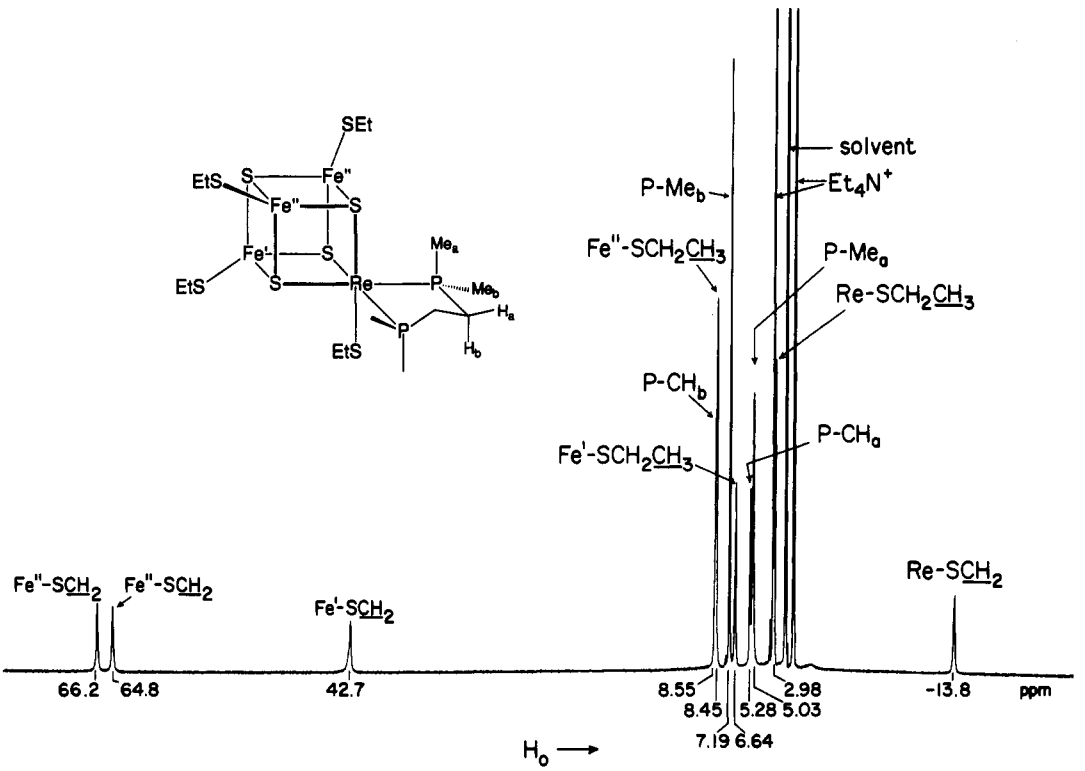

Figure 4. ^{1}H NMR spectrum of cluster **4** in CD_3CN solution at 297 K. Signal assignments are indicated.

Table IV. Magnetic and Mössbauer Properties of $[ReFe_3S_4(SEt)_4(dmpe)]^-$

Curie–Weiss range, K	7–50
C, (emu K)/G	3.279
Θ, K	−0.858
S	2
μ_{eff}, μ_B	5.12
μ_{eff}, μ_B (300 K)	4.53
D, cm^{-1}	6.82
$\lvert E/D \rvert$	0.07
δ,[a,b] mm/s (4.2, 80 K)	0.37, 0.36 (2) 0.38, 0.37 (1)
ΔE_Q.[b,c] mm/s (4.2, 80 K)	1.39, 1.34 (2) 1.07, 1.13 (1)

[a] Value vs Fe metal at 4.2 K, ±0.02 mm/s. [b] In parentheses are reported the relative intensities of the doublets. [c] ±0.03 mm/s.

and are considered to signify an oxidation state no lower than $Fe^{2.50+}$.

Magnetism and Ground State. The magnetic susceptibility of cluster **4** was examined in the 6–300 K interval at 5 kOe and the magnetization behavior at 1.8–100 K in applied fields up to 50 kOe. Plots of the data are shown in Figure 3; good fits to the data were obtained with use of the parameters summarized in Table IV. The Curie constant C was obtained by fitting the data to the Curie–Weiss law at 7–50 K and is compatible with g = 2.09 and S = 2.

Magnetization measurements were performed to determine additional features of the ground state. The magnetization behavior was found to be field-dependent, thus indicating the presence of zero-field splitting. A fit of the data at three applied fields was performed with use of the Hamiltonian 1 with S = 2

$$\mathbf{H} = D[S_z^2 - S(S+1)/3] + E(S_x^2 - S_y^2) + g_e\mu_B H\cdot S \qquad (1)$$

and a simplex algorithm that allowed simultaneous fits of the data at the three fields. Parameters obtained from the fits are given in Table IV. These results conclusively demonstrate that the $[ReFe_3S_4]^{3+}$ core of cluster **4** has a spin quintet ground state.

Mössbauer Properties. The Mössbauer spectra of **4** were examined at 4.2 and 80 K in zero applied field. At 80 K, the cluster exhibits a broad symmetric quadrupole doublet, which becomes somewhat asymmetric at 4.2 K. Least-squares fits to the data were performed at both temperatures assuming a 2:1 site ratio, consistent with idealized C_s symmetry. Parameters derived from the fits are included in Table IV.

Isomer shifts indicate an essentially uniform distribution of electron density over the two sites and the absence of trapped-valence Fe^{II} and Fe^{III}, whose isomer shifts would be ca. 0.2 and 0.6 mm/s,[35] respectively. Values of the isomer shift at 4.2 K are related to the mean oxidation state s of Fe atoms in the cluster by the empirical relationship δ = 1.44 − 0.43s.[36] The shift indicates a mean oxidation state of ca. 2.50+, suggesting an effective rhenium oxidation state of 3+ to 4+. These estimates are consistent with the structural results above.

Solution Structure. The paramagnetism of **4** affords an isotropically shifted ^{1}H NMR spectrum, shown in Figure 4, which is much better resolved than that of the related molybdenum cluster **5**. Signal assignments have been established by 2D COSY experiments and relative intensities, together with comparisons of previously assigned $MoFe_3S_4$ cluster species.[18,22,23] The spectrum corresponds to effective C_s symmetry, with two inequivalent sites, Fe′ and Fe″. The two equally intense signals centered at 65 ppm and split by 1.4 ppm must arise from the diastereotopic Fe″–SCH_2 protons; the Fe′–SCH_2 resonance is a singlet at 42.7 ppm. The dmpe resonances consist of two methyl and two methylene signals (a, b) owing to the axial and equatorial dispositions of these groups, which remain inequivalent upon rapid interchange of enantiomeric skew conformations.

Electron-Transfer Properties. The cyclic voltammogram of cluster **4** in acetonitrile is shown in Figure 5. Two electrochemically reversible processes are observed, defining the three-member electron-transfer series 2, specified in terms of core

$$[ReFe_3S_4]^{4+} \underset{-0.31\ V}{\overset{E_1}{\rightleftharpoons}} [ReFe_3S_4]^{3+} \underset{-1.18\ V}{\overset{E_2}{\rightleftharpoons}} [ReFe_3S_4]^{2+} \qquad (2)$$

$$[ReFe_3S_4]^{4+} + [ReFe_3S_4]^{2+} \overset{K_{com}}{\rightleftharpoons} [ReFe_3S_4]^{3+} \qquad (3)$$

charges, with the indicated potentials. Coulometry of step E_2

(35) (a) Lane, R. W.; Ibers, J. A.; Frankel, R. B.; Papaefthymiou, G. C.; Holm, R. H. *J. Am. Chem. Soc.* **1977**, *99*, 84. (b) Coucouvanis, D.; Swenson, D.; Baenziger, N. C.; Murphy, C.; Holah, D. G.; Sfarnas, N.; Simopoulos, A.; Kostikas, A. *J. Am. Chem. Soc.* **1981**, *103*, 3350.
(36) Christou, G.; Mascharak, P. K.; Armstrong, W. H.; Papaefthymiou, G. C.; Frankel, R. B.; Holm, R. H. *J. Am. Chem. Soc.* **1982**, *104*, 2820.

Table V. Comparative Structural Properties of MFe_3S_4 (M = V, Mo, Re, Ni) Synthetic Single Cubanes and Protein-Bound $[Fe_3S_4]^+$ Voided-Cubane Clusters

cluster	M···Fe[a]	M–S[a]	Fe···Fe[a]	Fe–S[a]	M–P[a]	M–SR[a]	Fe–SR[a]	ref
$[VFe_3S_4Cl_3(dmpe)(MeCN)]^-$	2.72 (2)	2.32 (6)	2.72 (5)	2.28 (2)	2.500 (6)			5
$[MoFe_3S_4(SEt)_4(dmpe)]^{-b}$	2.75 (3)	2.37 (2)	2.71 (1)	2.26 (2)	2.502 (5)	2.486 (8)	2.25 (1)	18
	2.72 (1)	2.37 (2)	2.726 (8)	2.27 (2)	2.59 (3)	2.566 (8)	2.25 (2)	
$[ReFe_3S_4(SEt)_4(dmpe)]^{-b}$	2.79 (1)	2.389 (6)	2.72 (3)	2.26 (3)	2.413 (7)	2.418 (1)	2.254 (2)	*c*
	2.758 (7)	2.36 (2)	2.72 (1)	2.27 (1)	2.492 (3)	2.536 (1)	2.24 (1)	
$[NiFe_3S_4(SEt)_3(PPh_3)]^{2-}$	2.69 (2)	2.262 (6)	2.75 (2)	2.29 (2)	2.174 (6)		2.283 (6)	15
$[Fe_3S_4]^+$ *Dg* Fd II[d]			2.75	2.27			2.24	37
			2.72–2.77[e]	2.22–2.32[e]			2.16–2.30[e]	
$[Fe_3S_4]^+$, aconitase[f]			2.69	2.30			2.32	38
			2.64–2.73[e]	2.25–2.35[e]			2.28–2.34[e]	

[a] Mean distances (Å). The standard deviation of the mean was estimated from $\sigma \cong s = [(|\sum x_i^2 - nx^2|)/(n-1)]^{1/2}$. [b] The two sets of distances refer to two independent anions. [c] This work. [d] Structure solved at 1.7-Å resolution (*Dg* Fd II = *Desulfovibrio gigas* ferredoxin II). [e] Range of observed distances. [f] Structure solved at 2.5-Å resolution.

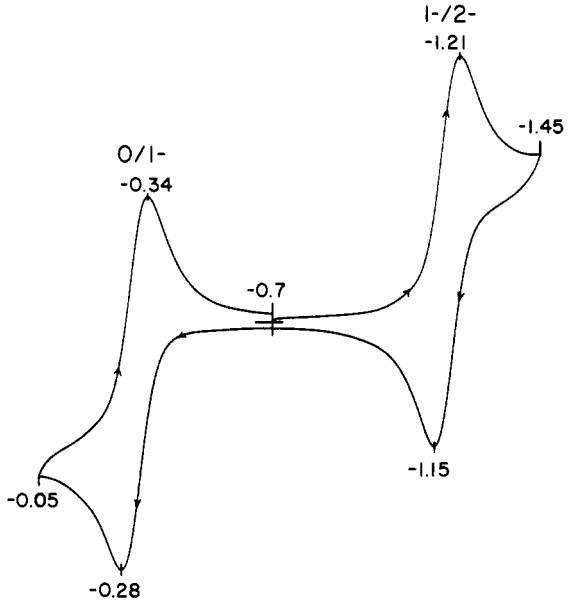

Figure 5. Cyclic voltammogram of cluster **4** in acetonitrile solution at room temperature. Peak potentials vs SCE are indicated.

demonstrated it to be a one-electron process. The fully oxidized cluster in step E_1 was not stable on the coulometric time scale of ca. 15 min., over which an irreversible multielectron oxidation was observed. The potential separation of 0.87 V ensures the stability of the $[ReFe_3S_4]^{3+}$ core in solution inasmuch as $K_{com} = 10^{14.7}$ for reaction 3. The $[ReFe_3S_4]^{3+}$ state has already been isolated in the form of double-cubanes **1** and **2**.[16,17] We have been unable to isolate the terminal oxidized member of series 2. However, the $[ReFe_3S_4]^{4+}$ state has been obtained as the double cubane **3**.[16,17] The terminal reduced member of series 2 has been produced only by electrochemical reduction at potentials ≤ 1.1 V.

General Considerations of Heterometal Cubane Clusters. We offer here some considerations of these clusters, which include and extend beyond the $ReFe_3S_4$ species examined in this and previous work.[16,17] Among such clusters are **6–13**, which are depicted in Figure 6 together with reactions 4 and 5, to which we will return.

(a) Comparisons of MFe_3S_4 Clusters (M = V, Mo, Re, Ni). In Table V are collected the main structural features of single-cubane clusters containing these heterometals, from which it is evident that all clusters have analogous structures. The Fe–Fe and Fe–S distances have a smaller dependence on heterometal M than do the M–Fe, M–S, and Fe–SR distances and are comparable to the less precisely known values for the cuboidal protein-bound Fe_3S_4 clusters **10**.[37,38] The terminal Fe–SR bond lengths respond to changes in the mean oxidation state of the iron

Table VI. Core Oxidation States in Isolated Clusters and Proteins

core	*S*	ref
$[Fe_3S_4]^{+,0}$ (**10**)	1/2, 2	37, 38, 45
$[VFe_3S_4]^{2+}$ (**6**, **7**)	3/2	5, 44
$[MoFe_3S_4]^{3+,2+}$ (**5**)	3/2, 2	2, 3, 36, 44, 46
$[WFe_3S_4]^{3+}$ (**6**, **7**)	*a*	3, 4
$[ReFe_3S_4]^{4+,3+}$ (**1–4**)	3/2, 2	16, 17, *b*
$[FeFe_3S_4]^{2+}$ (**8**)	2	40
$[CoFe_3S_4]^{2+,+}$ (**11**[c])	1/2, >0	11
$[NiFe_3S_4]^{2+}$ (**9**, **11**[c])	3/2	12, 15
$[ZnFe_3S_4]^+$ (**11**[c])	5/2	13, 14
$[CdFe_3S_4]^+$ (**11**[c])	5/2	14

[a] Not determined. [b] This work. [c] Protein-bound cluster.

atoms, becoming longer as the oxidation state approaches Fe^{2+}.

The potential for the redox couple $[MoFe_3S_4(SEt)_4(dmpe)]^{-,2-}$ (**5**; −1.41 V[18]) is about 1 V more negative than for the isoelectronic couple $[ReFe_3S_4(SEt)_4(dmpe)]^{0,-}$ (**4**; −0.31 V) in the identical ligand environment. This difference is primarily an effect of the larger negative charge on the molybdenum cluster. When cluster charges of isoelectronic couples are the same, as with $[VFe_3S_4Cl_3(dmpe)(MeCN)]^{-,2-}$ (**6**; −1.28 V[5]) and $\mathbf{5}^{-,2-}$ (the closest comparison available), the difference diminishes to 0.13 V. Inasmuch as chloride tends to increase potentials relative to thiolate, this difference would be smaller if **6** contained thiolate ligands.

With the crystallographic proof of structure **10**, which has the configuration of a site-voided cubane, and detailed interpretation of the Mössbauer spectra of Fe_3S_4 clusters in proteins, it becomes more meaningful than heretofore to estimate charge distributions in MFe_3S_4 cores. Series 6 conveys the known oxidation states and isomer shifts[39] (mm/s; 4.2 or 77 K) of the Fe_3S_4 core. This information comes entirely from protein-bound $Fe_3S_4(S\text{-}Cys)_3$ clusters inasmuch as **10** has yet to be synthesized as a stable species. The fully oxidized form is that normally isolated. It is reducible to $[Fe_3S_4]^0$, whose unusual electronic structure consists of a localized high-spin Fe^{3+} site and a delocalized pair.[39b] The indicated mean isomer shift is essentially independent of the presence of a fourth metal atom, as shown by results for cluster **8**, whose unique site contains low-spin Fe^{2+},[40] and for oxidized protein cluster **11**–Co.[11] The terminal reduced form has not been obtained as such in any protein[41] but has been stabilized in the reduced protein cluster **11**–Zn.[13,14]

(37) Kissinger, C. R.; Adman, E. T.; Sieker, L. C.; Jensen, L. H. *J. Am. Chem. Soc.* **1988**, *110*, 8721.
(38) Robbins, A. H.; Stout, C. D. *Proc. Natl. Acad. Sci. U.S.A.* **1989**, *86*, 3639; *Proteins* **1989**, *5*, 289.
(39) (a) Huynh, B. H.; Moura, J. J. G.; Moura, I.; Kent, T. A.; LeGall, J.; Xavier, A. V.; Münck, E. *J. Biol. Chem.* **1980**, *255*, 3242. (b) Papaefthymiou, V.; Girerd, J.-J.; Moura, I.; Moura, J. J. G.; Münck, E. *J. Am. Chem. Soc.* **1987**, *109*, 4703. (c) Emptage, M. H.; Kent, T. A.; Huynh, B. H.; Rawlings, J.; Orme-Johnson, W. H.; Münck, E. *J. Biol. Chem.* **1980**, *255*, 1793. (d) Kent, T. A.; Dreyer, J.-L.; Kennedy, M. C.; Huynh, B. H.; Emptage, M. H.; Beinert, H.; Münck, E. *Proc. Natl. Acad. Sci. U.S.A.* **1982**, *79*, 1096.
(40) (a) Weigel, J. A.; Holm, R. H.; Surerus, K. K.; Münck, E. *J. Am. Chem. Soc.* **1989**, *111*, 9246. (b) Weigel, J. A.; Srivastava, K. K. P.; Day, E. P.; Münck, E.; Holm, R. H. *J. Am. Chem. Soc.* **1990**, *112*, 8015.
(41) Recent evidence indicates that for at least one protein (*Desulfovibrio africanus* ferredoxin III) the $[Fe_3S_4]^0$ level is reduced in a $2e^-/2H^+$ process: Armstrong, F. A.; Butt, J. N.; George, S. J.; Hatchikian, E. C.; Thomson, A. J. *FEBS Lett.* **1989**, *259*, 15.

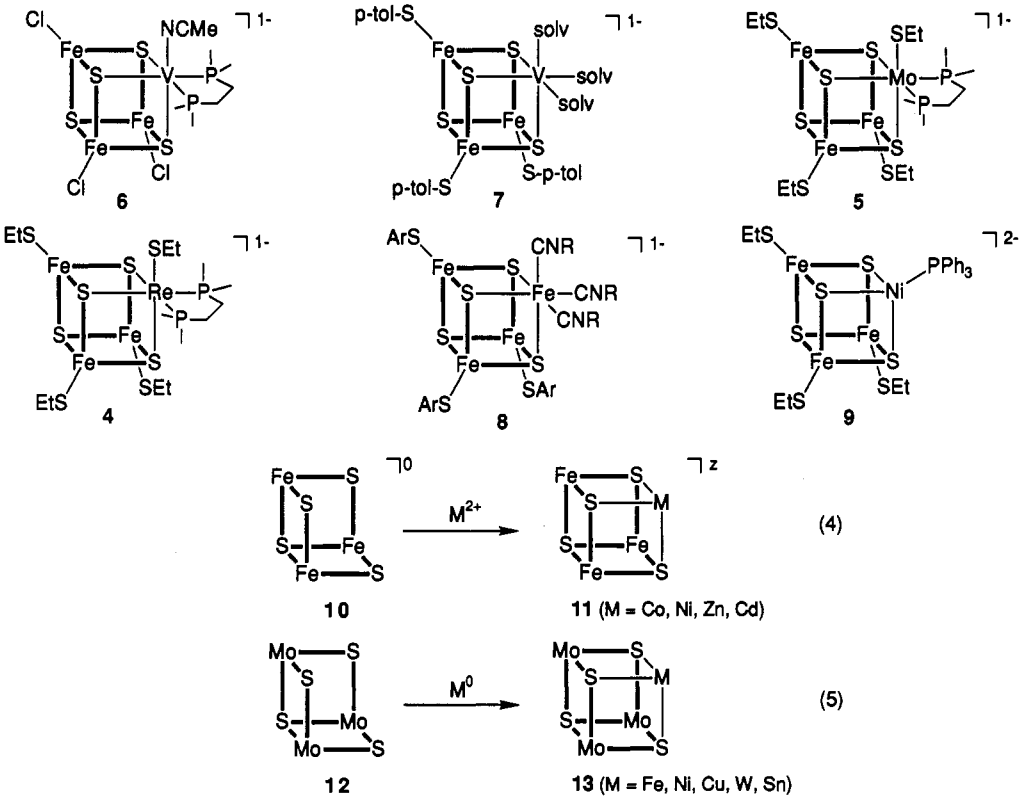

Figure 6. Schematic depiction of cubane-type clusters **4–9** and of heterometal incorporation reactions 4 and 5, which make clear the function of units **10** and **12** as quasi-rigid cluster ligands.

$$\underset{0.15\ (Fe^{3+})}{[Fe_3S_4]^{+}} \rightleftharpoons \underset{\substack{0.18\ (Fe^{3+})\\ 0.34\ (Fe^{2.5+})\\ 0.29\text{–}0.30\ (Fe^{2.67+})}}{[Fe_3S_4]^{0}} \rightleftharpoons \underset{0.43\ (Fe^{2.33+})}{[Fe_3S_4]^{-}} \quad (6)$$

Series 7–9 summarize a large body of Mössbauer data in terms of mean isomer shifts for the indicated core oxidation states of structurally analogous species. Comparisons between series are

$$\underset{0.28\ mm/s}{[MoFe_3S_4]^{3+}} = \underset{0.32\ mm/s}{[WFe_3S_4]^{3+}} \quad \underset{0.33\ mm/s}{[ReFe_3S_4]^{3+}}\ (\mathbf{1}) \quad (7)$$

$$\underset{0.30\ mm/s}{[MoFe_3S_4]^{3+}} = \underset{0.33\ mm/s}{[WFe_3S_4]^{3+}} = \underset{0.25\ mm/s}{[ReFe_3S_4]^{4+}}\ (\mathbf{3}) \quad (8)$$

$$[VFe_3S_4]^{2+}\ (\mathbf{7}) = 0.33\ mm/s$$

$$\underset{0.28\ mm/s}{[MoFe_3S_4]^{3+}}\ (\mathbf{5}) \quad \underset{0.38\ mm/s}{[ReFe_3S_4]^{3+}}\ (\mathbf{4}) \quad \underset{0.35\ mm/s}{[NiFe_3S_4]^{+}}\ (\mathbf{9}) \quad (9)$$

less meaningful owing to structural and ligation differences. Series 7 contains the triply bridged double cubanes $[M_2Fe_6S_8(SEt)_9]^{3-}$[42] of structure **1**, series 8 the Fe^{II}-bridged double cubanes $[M_2Fe_7S_8(SR)_{12}]^{4-,2-}$[43] of structure **2/3**, and series 9 the single cubanes. Isoelectronic species are connected by an equals sign. Upon comparison with series 6, it is immediately evident that the Fe_3S_4 portions of all clusters are reduced *below* the uniform Fe^{3+} level of $[Fe_3S_4]^{+}$. Further, the extent of reduction is variable, with the two Re-containing cores being at or near the extremes of oxidation and reduction of the Fe_3S_4 portions of the clusters. In certain cases, the isomer shifts sensibly define the oxidation levels of these portions and lead by difference to an effective oxidation state of the heterometal. Thus, the $[MFe_3S_4]^{3+}$ (M = Mo, W) core would appear to contain $[Fe_3S_4]^{0}$, indicating an oxidation state near M^{3+}. Similarly, the effective vanadium oxidation state in cluster **7** is in the $V^{2+,3+}$ range. The $[ReFe_3S_4]^{3+}$ core of single-cubane **5** is within the limits $[Fe_3S_4]^{0/1-} + Re^{3+/4+}$, consistent with the structural data above. The Ni-containing cluster **9** contains a relatively highly reduced Fe_3S_4 portion also, a matter reflected in its comparatively long Fe–SR distance (Table V). For the most part, these and other conclusions that may be drawn from series 6–9 for V, Mo, and W clusters are consistent with those made previously, which were taken from a combination of structural evidence and an empirical relationship between oxidation state and isomer shift.[2,3,36,44]

While charge distributions obtained in this way reflect s-electron densities and cannot be highly precise, they are nonetheless useful in a relative sense with regard to certain electronic and reactivity features. For example, upon the reduction of double-cubane $[Mo_2Fe_6S_8(SPh)_9]^{3-}$ to $[Mo_2Fe_6S_8(SPh)_9]^{5-}$ the isomer shift increased by 0.11–0.12 mm/s at 4.2 K.[36] With the availability of the data in series 6, it is now clear, on direct experimental grounds, that the majority of added electron density is absorbed by the Fe_3S_4 cluster portion and the effective molybdenum oxidation state remains at or near Mo^{3+}.

(b) The Fe_3S_4 Cluster as Ligand. In closing, we note the impressive and increasing scope of MFe_3S_4 cubane clusters, which now includes some eight heterometals. All known examples in isolated synthetic compounds and in proteins are collected in Table VI,[47] together with their ground state spins. Clusters **1–7** have

(42) (a) Wolff, T. E.; Berg, J. M.; Hodgson, K. O.; Frankel, R. B.; Holm, R. H. *J. Am. Chem. Soc.* **1979**, *101*, 4140. (b) Christou, G.; Garner, C. D.; Miller, R. M.; Johnson, C. E.; Rush, J. D. *J. Chem. Soc., Dalton Trans.* **1980**, 1980.

(43) Wolff, T. E.; Power, P. P.; Frankel, R. B.; Holm, R. H. *J. Am. Chem. Soc.* **1980**, *102*, 4694.

(44) Carney, M. J.; Kovacs, J. K.; Zhang, Y.-P.; Papaefthymiou, G. C.; Spartalian, K.; Frankel, R. B.; Holm, R. H. *Inorg. Chem.* **1987**, *26*, 719.

(45) Day, E. P.; Peterson, J.; Bonvoisin, J. J.; Moura, I.; Moura, J. J. G. *J. Biol. Chem.* **1988**, *263*, 3684.

(46) Mascharak, P. K.; Papaefthymiou, G. C.; Armstrong, W. H.; Foner, S.; Frankel, R. B.; Holm, R. H. *Inorg. Chem.* **1983**, *22*, 2851.

(47) Arbitrarily not included in Table VI is the cluster $[MoFe_3S_4(SEt)_3(CO)_3]^{3-}$.[48] While it is a MFe_3S_4 cluster, the $Mo(CO)_3$ fragment is rather weakly bound to the Fe_3S_4 portion (Mo–S = 2.62–2.64 Å, Mo–Fe = 3.22–3.27 Å), in contrast to the tight integration of metal in the clusters of, e.g., Table V.

(48) Coucouvanis, D.; Al-Ahmad, S.; Salifoglou, A.; Dunham, W. R.; Sands, R. H. *Angew. Chem., Int. Ed. Engl.* **1988**, *27*, 1353.

been synthesized in self-assembly systems whose components generate in effect a redox potential that sets the oxidation state of the product cluster. This behavior is delicately balanced for double-cubanes **1-3** whose redox potentials (-0.2 to -0.8 V[16,17]) are easily reached, and more than one cluster may be obtained from very similar assembly systems. Because the sulfur atoms of Fe_3S_4 are derived from the $[MS_4]^{z-}$ reactant and require (at least) one M-S bond rupture, the concept of this unit as a ligand is unconventional because it is not obviously preformed prior to incorporation of the heterometal. However, in reaction 4 (Figure 6) this is not the case with protein-bound cuboidal cluster **10**, which binds the indicated metal ions. While there is no crystallographic proof, spectroscopic features of the products indicate the incorporation of the metals into a cluster structure, very likely **11**.[11-15] As shown elsewhere,[15] the structure of **11**-Ni must resemble that of the cubane cluster **9**. The latter cluster was prepared by the reaction of linear $[Fe_3S_4(SEt)_4]^{3-}$ and $Ni(PPh_3)_3$.[15] In this case, the putative ligand is generated by a reductive isomerization.

The only other process involving a preformed cuboidal cluster as a ligand is reaction 5, in which the precursors contain the $[Mo_3S_4]^{4+}$ core **12**. Reduction to the $[Mo_3S_4]^{3+}$ or lower oxidation state is required for incorporation of the heterometal, which affords the structurally proven cubane-type clusters **13**.[49-51] One of these contains the $[Mo_3FeS_4]^{4+}$ core,[49a] with a metal site population that is the inverse of clusters such as **5**. Similarity, reaction 4 succeeds only if the $[Fe_3S_4]^{+}$ oxidation state is reduced with dithionite. The need for reduction in both cases appear to be analogous. It is probable that the sulfur atoms are not sufficiently electron-rich and polarizable to bind other metals when subjected to the demands of three highly electrophilic Fe^{3+} or Mo^{4+} atoms. Consequently, *reduced* Fe_3S_4 units such as those demonstrated in series 7-9 would appear to be essential to the tight incorporation of a M^{z+} heterometal in a cubane structure, regardless of the method of synthesis. We propose that the Fe_3S_4 unit be considered a *quasi-rigid cluster ligand*, whose effective oxidation state lies between 0 and 1- when bound to a fourth metal atom and whose internal structural features and electronic distributions are largely unchanged upon binding of a heterometal atom. A similar description applies to the Mo_3S_4 unit.

Current efforts are directed toward the extension of the synthetic MFe_3S_4 series, including biological metals,[15] and means of stabilization of the voided-cubane structure **10** outside a protein matrix.

Acknowledgment. This research was supported by NIH Grant GM 28856. X-ray equipment was obtained through NIH Grant 1 S10 RR 02247. We thank Dr. G. C. Papaefthymiou for use of a Mössbauer spectrometer and useful discussions.

Supplementary Material Available: For $(Et_4N)[ReFe_3S_4(SEt)_4(dmpe)]$, tables of crystallographic data, intensity collection and structure refinement parameters, positional and thermal parameters, and calculated hydrogen atom positions and a figure of the two independent clusters (11 pages); a listing of observed and calculated structure factors (37 pages). Ordering information is given on any current masthead page.

(49) (a) Shibahara, T.; Akashi, H.; Kuroya, H. *J. Am. Chem. Soc.* **1986**, *108*, 1342; *J. Coord. Chem.* **1988**, *18*, 233. (b) Shibahara, T.; Akashi, H.; Kuroya, H. *J. Am. Chem. Soc.* **1988**, *110*, 3313. (c) Akashi, H.; Shibihara, T. *Inorg. Chem.* **1989**, *28*, 2906.
(50) (a) Deeg, A.; Keck, H.; Kruse, A.; Kuchen, W.; Wunderlich, H. *Z. Naturforsch.* **1988**, *43b*, 1541. (b) Keck, H.; Kruse, A.; Mootz, D.; Wiskemann, R.; Wunderlich, H. *Z. Naturforsch.* **1990**, *45b*, 508.
(51) Wu, X.; Lu, S.; Zu, L.; Wu, Q.; Lu, J. *Inorg. Chim. Acta* **1987**, *133*, 39.

Contribution from the Department of Chemistry and Laboratory for Molecular Structure and Bonding, Texas A&M University, College Station, Texas 77843

Synthesis and Characterization of $Mo_2(OC_6F_5)_4(PMe_3)_4$

F. A. Cotton* and K. J. Wiesinger

Received August 2, 1990

The synthesis and molecular structure of $Mo_2(OC_6F_5)_4(PMe_3)_4$ (**1**) are reported. The synthesis involves the alcoholysis of $Mo_2(CH_3)_4(PMe_3)_4$ by C_6F_5OH to form **1** and CH_4(g). Compound **1** adopts a structural type that has not yet been seen for $Mo_2X_4L_4$ species. Crystal data for **1** are as follows: space group $P\bar{1}$, a = 11.368 (3) Å, b = 13.094 (3) Å, c = 10.574 (2) Å, α = 109.30 (2)°, β = 107.26 (2)°, γ = 95.01 (2)°, V = 1388 (1) Å^3, and Z = 1.

Introduction

For a molecule of the composition $M_2X_4L_4$, with a multiply bonded M_2 unit, a number of isomers are possible. By employment of a numbering scheme that was briefly mentioned in an earlier paper,[1] these isomers may be systematically and rigorously enumerated. The numbering scheme for a square-prismatic structure with a vertical M_2 axis is shown in Figure 1, along with a list of $M_2X_4L_4$ isomers. Pairs of isomers coupled by braces are enantiomorphs.

There are altogether ten geometric isomers, three of which are chiral and include enantiomorphs, to give a total of thirteen. Of these, four have unequal numbers of each kind of ligand at each end, viz., 4 vs 0 or 3 vs 1. In this group there is but one example of the 1,2,3,4-type. No example of any 3 vs 1 type has been reported.

Of the remaining six types of geometrical isomers, four have been observed. The 1,3,6,8-type is overwhelmingly the most common, and all the $Mo_2X_4(PR_3)_4$ molecules with X = halide,[2] CH_3,[3] NCS,[4] and NCO[4] are of this type. It is doubtless favored in these cases by the simple steric effect of the large PR_3 ligands avoiding adjacent positions. This tendency of the larger neutral ligands to occupy alternate vertices can be overcome by the use of bi- or multidentate ligands, thus allowing the isolation of species with (1,2,5,8/1,2,6,7), (1,2,7,8), and (1,3,5,7) distributions.

In this paper we report the first example of a 1,2,7,8 isomer in which all ligands are unidentate, namely $Mo_2(OC_6F_5)_4(PMe_3)_4$. A few other $M_2X_4L_4$ species in which X is an alkoxide have previously been reported, namely those listed in Table I. Five

* To whom correspondence should be addressed.

(1) Cotton, F. A.; Price, A. C.; Vidyasagar, K. *Inorg. Chem.* **1990**, *29*, 5143.
(2) Cotton, F. A.; Walton, R. A. *Multiple Bonds Between Metal Atoms*; John Wiley & Sons: New York, 1982.
(3) (a) Cotton, F. A.; Wiesinger, K. J. *Inorg. Chem.* **1990**, *29*, 2594. (b) Girolami, G. S.; Mainz, V. V.; Andersen, R. A.; Vollmer, S. H.; Day, V. W. *J. Am. Chem. Soc.* **1981**, *103*, 3953. (c) Andersen, R. A.; Jones, R. A.; Wilkinson, G. *J. Chem. Soc., Dalton Trans.* **1978**, 446.
(4) Cotton, F. A.; Matusz, M. *Inorg. Chem.* **1988**, *27*, 2127.
(5) Chisholm, M. H.; Folting, K.; Huffman, J. C.; Tatz, R. J. *J. Am. Chem. Soc.* **1984**, *106*, 1153.
(6) Coffindaffer, T. W.; Niccolai, G. P.; Powell, D.; Rothwell, I. P.; Huffman, J. C. *J. Am. Chem. Soc.* **1985**, *107*, 3572.

0020-1669/91/1330-0750$02.50/0